Sonochemical Synthesis of Two Novel Pb(II) 2D Metal Coordination polymer Complexes: New Precursor for Facile Fabrication of Lead(II) Oxide/Bromide Micro-Nanostructures

Payam Hayati [a, c], Salvio Suárez-García[c], Angel Gutierrez[d], Daniel Ruiz Molina[c*], Ali Morsali [b*], Ali Reza Rezvani[a*]

[a] Department of Chemistry, Faculty of Sciences, University of Sistan and Baluchestan, P.O. Box 98135-674, Zahedan, Iran.

[b]Department of Chemistry, Faculty of Sciences, Tarbiat Modares University, P.O. Box 14115-4838, Tehran, Islamic Republic of Iran.

[c]Catalan Institute of Nanoscience and Nanotechnology (ICN2), CSIC and BIST, Campus UAB, Bellaterra, 08193 Barcelona, Spain

[e]Departamento de Quimica Inorganica I Facultad de Ciencias Quimicas Universidad Complutense 28040-Madrid Spain.

Abstract

Two new lead(II) coordination polymer compounds (CSCs) (2D), $[Pb_2(L)_2(Br)_2]_n \cdot H_2O$ **(1)**, $[Pb_2(HL^{/})(L^{/})(H_2O)_2]_n \cdot H_2O$ **(2)**, where L= $C_6H_5NO_2$ (2-pyridinecarboxylic acid) and $L^{/}$= $C_9H_6O_6$ (1,3,5-tricarboxylic acid), have been synthesized under different experimental conditions. Micrometric crystals (bulk) or microsized materials have been obtained depending on using the branch tube method or sonochemical irradiation. All materials have been characterized by scanning electron microscopy (SEM) and powder X-ray diffraction (PXRD), FT-IR spectroscopy. Single crystal X-ray analyses on compounds **1** and **2** show that Pb^{2+} ions are 8-coordinated, 7 and 9-coordinated, respectively. Topological analysis shows that the compound **1** to **2** are 4,6L26, and **bnn** net, respectively. However, neither the shape nor the morphology is maintained, showing the role of sonochemistry to modulate both morphology and dimensions of

the resulting crystalline material, independently of whether we have a 2D coordination polymer. Finally, micro/structuration of lead(II) bromide oxide and lead(II) oxide have been prepared by calcination of two different lead (II) CPs at 700 °C that were characterized by scanning electron microscopy (SEM) and X-ray powder diffraction (XRD).

Keywords: Coordination polymer compounds, Sonochemical process, Ultrasound irradiation, Nano particle, Topology, Morphology.

1. Introduction

Coordination polymer compounds (CSCs) are presently of considerable interest and importance because of the scope they offer for the generation by design of new materials with a range of potentially useful properties [1,4]. Some very interesting types of CSCs with cyclic structures based on the concept of molecular squares using metal ions and bridging ligands containing N-donors including 4,4′-bipyridine, 4,4′-trimethyllenedipyridine, 1,2-bis(4-pyridyl)ethane, pyrazine, and related species have been reported [5-8]. Another strategy to obtain analogue coordination polymers with cavity or porosity structures is the reaction of metal ions with multifunctional ligands containing O-donors such as polycarboxylates. As a building block to create some porous or cyclic coordination polymer, trimesate (tma) ligand exhibits various coordination fashions and the capability of forming coordination architectures of diverse sizes and shapes. Although there were a lot of reports [9-12], on the infinite 1D, 2D, and 3D CSCs assembled by N and O donor ligands, up to now their functionalities remain, with the exception of several reports, largely unexplored. The CSCs of different metal ions could be synthesized through various methods, such as the diffusion-based method, layering technique, evaporation route, hydrothermal synthesis, crystallization technique and ultrasonic irradiation method [13-21]. Sonochemistry originates from the extreme transient conditions induced by ultrasound,

which produces unique hot spots that can perform temperatures above 5000 K, pressures exceeding 1000 atm, and heating and cooling rates in excess of 1010 K s^{-1}. These conditions are distinct from other conventional synthetic techniques for instance photochemistry, wet chemistry, hydrothermal synthesis or flame pyrolysis. The speed of sound in a typical liquid is 1000 to 1500 ms^{-1}, and ultrasonic wavelengths will vary from roughly 10 cm down to 100 mm on the frequency range of 20 kHz to 15 MHz, much larger than the molecular size scale. The chemical and physical effects of ultrasound therefore arise not from a direct interaction between chemical species and sound waves, but rather from the physical phenomenon of acoustic cavitation: the formation, growth, and implosive collapse of bubbles [22-26].

The synthesis of lead(II) systems is an increasingly active area due to presence of the $6s^2$ electron configuration and stereo activity with the valence shell lone electron pair and based on directed ligands classify as holodirected and hemidirected [27-33]. Lead possesses unique coordination versatilities with ligands and the synthesis of the related complexes at the nanoscale can open novel applications in the field of roofing, batteries and solder. So far, examples of $[Pb(NNO)_2]_n$, $[Pb(NNO)(SCN)]_n$ (HNNO = nicotinic acid *N*-oxide) [34] , $[Pb(\mu\text{-}L)(\mu\text{-}X)_2]_n$ (X = Cl,Br,I) (L=N,N′-bis(4-pyridylmethylidyne) phenylene-1,4-diamine [35], $[Pb(\mu\text{-bdabpm})(\mu\text{-}Br)_2]_n$ ([bdabpm = 1,4-Benzenediamine, N,N′-bis(3-pyridinylmethylene)]) [36], $\{[Pb_3(BOABA)_2(H_2O)]\cdot H_2O\}_n$, $\{[Pb_4(BOABA)_2(\mu_4\text{-}O)(H_2O)_2]\cdot H_2O\}_n$,($H_3BOABA$=3,5-bis-oxyacetate-benzoic acid) [37], $[Pb(\mu\text{-}4,4'\text{-bipy})(\mu\text{-}Br)_2]_n$, $[Pb(\mu\text{-bpa})(\mu\text{-}Br)_2]_n$, $[Pb(\mu\text{-bpe})(\mu\text{-}Br)_2]_n$, (4,4′-bipy= 4,4′-bipyridine, bpa= 1,2-bis(4-pyridyl)ethane) [38], $[Pb(\mu\text{-bpp})(\mu\text{-}Br)_2]_n$ (bpp = 1,3-di(4-pyridyl)propane) [39], $[Pb_2(\mu\text{-}I)_2(\mu\text{-dpp-}N,N,N,N)(\mu\text{-dpp-}N,N)I_2]n$ (dpp=2,3-bis(2-pyridyl)pyrazine) [40], $[Pb_2(TPAA)(HTPAA)(NO_3)]\cdot 6H_2O$, $[Pb_2(TPAA)(HTPAA)_2]\cdot DMF\cdot 0.5H_2O$ (DMF = N, N-Dimethylformamide, H_2TPAA=4-(1, 2, 4-

triazol-4-yl) phenylarsonic acid) (**2**) [41], rare lead (II) coordination supramolecular compounds with different ligand are reported. However, the synthesis of lead-based 2D coordination polymers still represents a challenge. In this manuscript, we have developed a simple sonochemical approach to prepare the novel lead(II) coordination polymers $[Pb(L)(SCN)]_n$ **(1)** and $[Pb_2(L^{/})_2(SCN)_4]_n$ **(2)** the resulting crystalline material is compared with that alternatively obtained by the branch tube methodology. Morphology was investigated and results compared with each other**.** Also, these compounds were used for preparation of $Pb_3O_2Br_2$ and PbO microparticles by using calcination process.

2. Experimental

2.1. Materials and physical techniques

Starting reagents for the synthesis were purchased and used without any purification from industrial suppliers (Sigma–Aldrich, Merck and others). Elemental analyses (carbon, hydrogen, and nitrogen) were performed employing a Heraeus Analytical Jena, Multi EA 3100 CHNO rapid analyzer. Fourier transform infrared spectra were recorded on a Bruker Tensor 27 FT-IR with a single window reflection of diamond ATR (Attenuated total reflectance) model MKII Golden Gate, Specac and the OPUS data collection programme software. The instrument is equipped with a room temperature detector, and a mid-IR source (4000 to 400 cm^{-1}). Since it is a single beam instrument, it was needed to run a background spectrum in air before the measurement. Single crystal X-ray diffraction experiments were carried out for compounds **1** and **2** with MoKα radiation (λ=0.71073 Å) at ambient temperature. A micro focused Rigaku mm003 source with integrated confocal caxFlux double bounce optic and HPAD Pilatus 200K detector were used for $Pb_3O_2Br_2$ and PbO (**(1-1, 1-2 , 1-3)** and **(2-1, 2-2, 2-3)**, respectively) while for two data were measured on a Bruker-Nonius Kappa CCD diffractometer. The structures were solved

by direct methods and refined by full matrix least squares on F^2. All non-hydrogen atoms were refined anisotropically. The hydrogen atoms were included with fixed isotropic contributions at their calculated positions determined by molecular geometry, except for the oxygen bonded hydrogen atoms, which were located on a difference Fourier map and refined riding on the corresponding atoms. (Computing details: data collection, cell refinement and data reduction: CrystalClear-SM expert 2.1b43 [42]; program(s) used to solve structure: SHELXT; program(s) used to refine structure: SHELXL-2014/7 [43]; molecular graphics: PLATON [44]; reduction of data and semiempirical absorption correction: SADABS program[45]; direct methods (SIR97 program[46]); full-matrix least-squares method on F^2: SHELXL-97 program [47] with the aid of the programs WinGX [48] and Olex2[49]). X-ray powder diffraction (XRD) measurements were performed using an X'pert diffractometer manufactured by Philips with monochromatized Cukα radiation and simulated XRD powder patterns based on single crystal data were prepared using the Mercury software. The samples were characterized with a scanning electron microscope (SEM) (FEI Quanta 650 FEG) in mode operation of secondary electrons (SE) with a beam voltage between 15 and 20 kV. The samples were prepared by deposition of a drop of the material previously dispersed properly solvents on aluminium stubs followed by evaporation of the solvent under ambient conditions. Before performing the analysis, the samples were metalized by depositing on the surface a thin platinum layer (5 nm) using a sputter coater (Leica EM ACE600). A multi wave ultrasonic generator (Elmasonic (Elma) S40 H), equipped with a converter/transducer and titanium oscillator (horn), 12.5 mm in diameter, operating at 20 kHz with a maximum power output of 400 W, was used for the ultrasonic irradiation.

2.2. Synthesis of $[Pb_2(L)_2(Br)_2]_n.H_2O$ (1) as single crystals by branch tube method

$Pb(NO_3)_2$ (1 mmol, 0.331g), 2-pyridinecarboxylic acid (L) (1 mmol, 0.123g) and KBr (2 mmol, 0.238g) were loaded into one arm of a branch tube and both of the arms were filled slowly by water. The chemical bearing arm was immersed in an oil bath kept at 60 °C. Crystals were formed on the inside surface of the arm kept at ambient temperature after. After 5 days, colorless crystals were deposited in the cooler arm were filtered off, washed with water and air dried. (0.198g, 47.93% yield based on final product), product **1** (single crystal): Anal. Calc. for $C_{12}H_8Br_2N_2O_4Pb_2 \cdot 0.5(H_2O)$: C: 17.46, H: 1.08, N:3.38 %; Found C: 17.35, H: 1.04, N:3.28 %. IR (selected bands for compound **1**; in cm^{-1}):3562(w), 3069(w), 1750(s), 1656(w), 1154(s).

2.3. Synthesis of $[Pb_2(L)_2(Br)_2]_n.H_2O$ (1) under ultrasonic irradiation

To prepare the microstructures of $[Pb_2(L)_2(Br)_2]_n$ (**2**) by sonochemical process, a high-density ultrasonic probe was immersed directly into the solution of $Pb(NO_3)_2$ (10 ml, 0.1 M) in water, then into this solution, a proper volume of KBr (10 ml, 0.1 M) and 2-pyridinecarboxylic acid (L) (10 ml, 0.1M) ligand in water solvent was added in a drop wise manner. The solution was irradiated by sonicate with the power of 60W, concentration of reactant 0.1M and temperature 30 °C for 30 min. For the study of the effect of time the initial reagents on size and morphology of nano- structured complex **1**, the above processes were done with 60 min and for the study of the effect of temperature with 60°C (time: 30 min, sonication power: 60W, concentration: 0.1M).

The obtained precipitates were filtered, subsequently washed with water and then dried.

Complex **1-1**: (0.290 g, 70.20% yield based on final product), product **1-1**: Anal. Calc. for $C_{12}H_8Br_2N_2O_4Pb_2 \cdot 0.5(H_2O)$: C: 17.46, H: 1.08, N:3.38 %; Found C: 17.29, H: 0.98, N:3.24 %.

IR (selected bands for compound **1-1**; in cm^{-1}): 3548(w), 3053(w), 1721(w), 1648(s), 1187(w), 705.51(s).

Complex **1-2**: (0.226 g, 54.71% yield based on final product), product **1-2**: Anal. Calc. for $C_{12}H_8Br_2N_2O_4Pb_2 \cdot 0.5(H_2O)$: C: 17.46, H: 1.08, N:3.38 %; Found C: 17.39, H: 1.01, N:3.30 %. IR (selected bands for compound **1-2**; in cm^{-1}): 3574(w), 3014(w), 1762w), 1632(s), 1169(w).

Complex **1-3**: (0.215 g, 52.04% yield based on final product), product **1-3**: Anal. Calc. for $C_{12}H_8Br_2N_2O_4Pb_2 \cdot 0.5(H_2O)$: C: 17.46, H: 1.08, N:3.38 %; Found C: 17.42, H: 1.06, N:3.18 %. IR (selected bands for compound **1-3**; in cm^{-1}): 3556(w), 3082(w), 1730(w), 1618(s), 1137(w).

2.4. Synthesis of $[Pb_2(HL^{/})(L^{/})H_2O]_n.H_2O$ (2) as single crystal by branch tube method

$Pb(NO_3)_2$ (0.5 mmol, 0.165 g), 1,3,5-benzentricarboxylic acid (H_3L) (0.5 mmol, 0.105 g) were loaded into one arm of a branch tube and both of the arms were filled slowly by water. The arm containing the reagents was immersed in an oil bath kept at 60 °C. After 12 days colorless crystals of **2** were formed on the inside surface of the arm kept at ambient temperature. They were filtered off, washed with water and air dried. (0.154 g, 34.92% yield based on final product), product **2** (single crystal): Anal. Calc. for $(C_{18}\ H_{11}\ O_{14}\ Pb_2)_n \cdot H_2O$: C: 24.44, H: 1.24, O: 25.34%; Found C: 24.36, H: 1.12 O: 24.68 %. IR (selected bands for compound 1; in cm^{-1}): 3560(br), 3105(br), 1696(s), 1533(s), 1362(w).

2.5. Synthesis of $[Pb_2(HL^{/})(L^{/})H_2O]_n.H_2O$ (2) under ultrasonic irradiation

A high-density ultrasonic probe was immersed directly into a water solution of 1,3,5-benzentricarboxylic acid (H_3L) (30 ml, 0.01 M), then into this solution, a proper volume of $Pb(NO3)2$ in water (30 ml, 0.01 M) was added in a drop wise manner. The solution was

irradiated by sonicate with the power of 60W, concentration of reactant 0.01M and temperature 30 °C for 30 min.

For the study of the effect of time the initial reagents on size and morphology of microstructured complex **2**, the above processes were done with 60 min and for the study of the effect of temperature with 60°C (time: 30 min, sonication power: 60W, concentration: 0.01M). The obtained precipitates were filtered, washed with water and dried in air.

Complex **2-1**: (0.198 g, 44.89% yield based on final product), product **2-1**: Anal. Calc. Anal. Calc. for $(C_{18}H_{11}O_{14}Pb_2)_n \cdot H_2O$: C: 24.44, H: 1.24, O: 25.34%; Found C: 24.19, H: 1.09 O: 25.18 %. IR (selected bands for compound 1; in cm^{-1}): 3550(br), 3101(br), 1680(s), 1522(s), 1358(w).

Complex **2-2**: (0.236 g, 53.49% yield based on final product), product **2-2** Anal. Calc. for $(C_{18}H_{11}O_{14}Pb_2)_n \cdot H_2O$: C: 24.44, H: 1.24, O: 25.34%; Found C: 24.37, H: 1.17 O: 25.22 %. IR (selected bands for compound **2-2**; in cm^{-1}): 3542(w), 3110(w), 1687(s), 1548(s), 1364(w).

Complex **2-3**: (0.208 g, 47.15% yield based on final product), product **2-3**: Anal. Calc. for $(C_{18}H_{11}O_{14}Pb_2)_n \cdot H_2O$: C: 24.44, H: 1.24, O: 25.34%; Found C: 24.37, H: 1.17 O: 25.22 %. IR (selected bands for compound **2-3**; in cm^{-1}): 3538(w), 3108(w), 1679(s), 1562(s), 1356(w).

2.6. Synthesis of $Pb_3O_2Br_2$ as nanoparticles by thermal decomposition of complex 1

The preparation of $Pb_3O_2Br_2$ calcinations of complex **1** was done at 700 °C in static atmosphere of air for 4 h. Powder XRD diffraction shows that calcination was completed and the entire complexes were decomposed.

2.7. Synthesis of PbO nanostructures by thermal decomposition of complex 2

Microparticles of complex **2** transferred to a crucible. The crucible was transferred to furnace and heated at 700 ºC under static atmosphere of air for 4 h. The furnace was cooled to 25ºC. The organic components were combusted and PbO microstructures were produced. The XRD pattern shows the product is PbO.

3. Results and discussion

A 2D CSCs $[Pb_2(L)_2(Br)_2]_n.H_2O$ **(1)** was obtained by reaction of L= $C_6H_5NO_2$ (2-pyridinecarboxylic acid), potassium bromide with lead(II) nitrate in water. The coordination polymer (CP) $[Pb_2(HL^{/})(L^{/})H2O]\cdot H2O$ **(2)**, was obtained by the reaction between the organic oxygen-donor ligand and lead(II) nitrate, which yielded in crystalline material formulated as new coordination polymer. Utilizing 1,3,5-tricarboxylic acid ($L^{/}$) ligand in lead (II) nitrate leads to formation of new molecular CP $[Pb_2(HL^{/})(L^{/})H_2O]_n.H_2O$ **(2)**. Microstructures of new complexes were obtained in aqueous solution by ultrasonic irradiation. Single crystals of new compounds, suitable for X-ray crystallography, were prepared by thermal gradient method applied to an aqueous and methanol solution of the reagents (the ‘‘branched tube method’’). Single crystal X-ray diffraction analysis (Tables 1- 3) of compounds **1** and **2** were carried out and the coordination environment of the title complexes are shown in (Fig .1) Single X-ray crystal analysis reveals that $[Pb_2(L)_2(Br)_2]_n\cdot H_2O$ **(1)**, and $[Pb2(HL^{/})(L^{/})H2O]_n\cdot H2O$ **(2)** complexes crystallize in monoclinic and triclinic space group ($P2_1/n$ and P_{-1}, respectively).

The Pb atoms of complex **1** coordinate two Br atoms, one O atom and one N atom composing distorted octahedral coordination NO_3Br_4 (Fig. 1). The asymmetric unit of compound **1** contains two Pb^{2+} cations, which coordinate two 2-pyridinecarboxylic acid ligand (L= $C_6H_5NO_2$), one

water molecule in water molecule lattice structure and two Br^- anions (Fig. 2). The crystal packing is composed of one crystallographically different [Pb(L)(Br)] units, labelled A, showing the same coordinative features and alternating along the *a*-crystal direction. Ligands are bridging neighboring lead atoms and the consecutive A units, giving rise to a 2D network. One L ligand, unit A, is coordinated in a chelating way with the nitrogen in the vertex of the pyramid and one oxygen atom in the basal plane. All the picolinate ligands show the same bridging-chelating coordination scheme leading to the formation of a one dimensional chain: …–Pb1–O3–Pb2–O1–Pb1–… along the crystal *a* axis. There is an additional Pb-Br interaction along the chain, with short contacts of 3.451 Å (Pb1–Br2) and 3.395(3) Å (Pb2–Br1) that are blocking the exposed coordinative position of the lead atoms (Fig 3, 4 and table 2). The coordination environment of the lead atoms is completed by two bromine atoms that are bridging Pb1 and Pb2 ions of different chains, thus extending the polymer along the *b*axis (Fig 5). Furthermore, there are hydrogen bound between O(4) and H(9) in each layer [H(9)-O(4) distance of 2.037 Å]. Additionally, H-bonds connect the layers in **1** into 3D (along (0,1,0) direction) framework. Obviously, hydrogen and $\pi - \pi$ interactions play major role in formation of the layer packaging (Fig. 6).

Simultaneously every 2-pyridinecarboxylic acid ligand and Br^- anion is bridging and coordinated by two Pb^{2+} cations. Coordination bonds form tetramer ring-shaped complex $[Pb_2(L)_2(Br)_2]_n \cdot H_2O$ (Fig.1 and 8). According to ToposPro package the underlying topology of the complex is **2,4L2**, which is abundant for 2D CP (more than 75 examples in TTO collection of ToposPro (Fig. 9) [50-51]. Every $[Pb_2(L)_2(Br)_2]_n.H_2O$ layer is surrounded by two other same complexes forming van-der-waals bonded and hydrogen bound (Fig. 9).

In complex **2**, Pb atoms are coordinated by seven and nine O atoms have pentagonal bipyramidal and triaugmented triangular prism structure and coordination sphere as O_7 and O_9, respectively (Fig.1). The asymmetric unit of compound **2** contains two Pb^{2+} cations, which coordinate two 1,3,5-tricarboxylic acid ligand and one H_2O molecule (Fig. 2). Each 1,3,5-tricarboxylic acid ligand in compound **2** is coordinated to two Pb atom by O atom of carbonyl and hydroxide group, and Pb–O distance is about 2.51-2.90Å (Table 3 and Fig. 3). Also, shows compound **2** is two-dimensional coordination polymer complex. For four Pb^{+2} cations, there are π-π interactions with each other. Four molecules contacts by two aromatic rings (L), in fact L is linker and connected by carboxylate groups. Obviously π-π interactions play major role in formation of the molecular by surrounding each molecule in hexagonal geometry of connection (Fig. 5). Hydrogen bound is formed between the hydrogen of molecular water and oxygen of the carboxylic group present in the ligand and is expanded along (1,0,0) direction. Therefore, there are $\pi - \pi$ interaction between aromatic rings which lead to crystal structure be stable (Fig. 7).

The coordination interactions can be separated in two groups:

i) Strong, more valence, in short range of 0.930-2.717Å;

ii) Weak, more electrostatic, in long range of 3.085-3.801Å.

Structures of compound **2** is two-periodic ((1,1,0) orientation) coordination polymer architectures, respectively. To understand the global topological motif for connection of ligands and metal atoms into periodic networks we performed topological analysis by program package ToposPro. For this goal the underlying net in standard representation was constructed [50]. Thus, the underlying net for compound **2** is represented by 3-coordinated nodes from HL and L ligands, as well as 7 and 9-coordinated Pb^{2+} ions. The 2D net belongs to topological type of **bnn**

hexagonal, Shubnikov plane net (Fig.8) [50-51]. Additionally, one H_2O molecule is coordinated to each Pb (II) cation with contacts distances Pb–O in the range of 2.61-2.94 Å (Table 3 and Fig. 3). 1,3,5-tricarboxylic acid ligand is located between two layer (2D) and is connected through O atoms carbonyl and hydroxide of carboxylic acid (functional group) (Fig. 9). Figure 10 shows a fragment of the 3D framework in complexes **1** and **2**.

The IR spectra display characteristic absorption bands for 2-pyridinecarboxylic acid ligand and H_2O in compounds and **1**. The relatively weak absorption bands to compound **1** about 3000 cm^{-1} result from the O-H stretching frequency carboxylic acid group ligand. The absorption bands with variable intensity in the frequency range 1700-1750 cm^{-1} correspond to C=O stretching frequency of the carbonyl from the 2-pyridinecarboxylic acid ligand. Also, the characteristic band of the C-O stretching frequency carboxylic acid group appears at 1000-1300 cm^{-1}. The IR spectrum of compound **1** shows the characteristic stretching frequency of H_2O group observed at around 3574 cm^{-1}. For compound **2** two bands around 1500-1700 cm^{-1} are due to the C=C stretching frequency amine group ligand. (Fig. 11).

For compound **2** the IR spectra display characteristic absorption bands for H_2O and the 1,3,5-benzentricarboxlic acid ligand in compound **2**. The relatively weak absorption bands to compound **2** about 3500 cm^{-1} result from the stretching frequency H_2O group. Additionally, the relatively weak absorption bands to compound **2** about 3000 cm^{-1} result from the O–H stretching frequency carboxylic acid group ligand. The absorption bands with variable intensity in the frequency range 1700–1750 cm^{-1} correspond to C=O stretching frequency of the carbonyl from the 1,3,5-benzentricarboxlic acid ligand. The absorption bands around 1448 and 825 cm^{-1} are related to stretching of C=C and =C-H bending of aromatic rings. Also, the characteristic band of the C-O stretching frequency carboxylic acid group appears at 1000-1300 cm^{-1}. In summary for

all compounds, the elemental analysis and IR spectra of the nano-structure produced by the sonochemical method as well as the bulk material produced by the branched tube method are indistinguishable (Fig. 12).

Ligand-free $Pb_3O_2Br_2$ and PbO microstructures were simply synthesized by solid-state transformation of compound **1** and **2** at 700°C under air atmosphere for 4 h. Figure 13 and 14 provide the XRD pattern of the residue obtained from the calcination of compound **1** and **2**. The obtained pattern matches with the standard patterns of $Pb_3O_2Br_2$ and PbO with the lattice parameters [a =12.252(3) Å, b =5.873(1), c =9.815(3) Å, S.G. = P_{nma} (61) and z = 4] and [a =5.8931(1) Å, b =5.4904(4), c =4.7528(1) Å, S.G. = P_{bcm} (57) and z = 4] which are the same as the reported values (Powder diffraction file 01-087-1185 and 01-077-1971 38-1477), respectively. As the calcination process was successful for the preparation of $Pb_3O_2Br_2$ and PbO, we used the nano-sized compounds **1** and **2** prepared by the sonochemical process at different conditions which is written in Table 4. For the two compounds, acceptable matches, with slight differences in 2θ, were observed between the simulated and experimental powder X-ray diffraction patterns. This indicates that the compound **1** and **2** obtained by the sonochemical which are initial material for preparing $Pb_3O_2Br_2$ and PbO structures. The SEM images of the microstructures obtained after the calcination are shown in Fig 15 and 16.

4. Conclusion

Two new Pb(II) CSCs, $[Pb_2(L)_2(Br)_2]_n \cdot H_2O$ **(1)** and $[Pb_2(HL')(L')(H_2O)_2]_n \cdot H_2O$ **(2)** have been synthesized by using a thermal gradient approach. Coordination polymers complexes **1** and **2** possess topology type and point symbol 4,6L26 and **bnn** net, {3^2.4^2.5^2}{3^4.4^4.5^4.6^3} and {4^6.6^4}, respectively. Larger crystals suitable for single crystal x-ray diffraction have been obtained by the branched tube method. Calcination method has been used to obtain

crystalline structures a few micron length width. Interestingly, the simulated x-ray diffraction powder obtained from the x-ray data confirms the structure of the microcrystal obtained by calcination method. These results confirm the potentially of ultrasound for the obtaining of microstructures of $Pb_3O_2Br_2$ and PbO.

Supplementary material

Crystallographic data for the structure reported in this paper have been deposited with the Cambridge Crystallographic Data Centre as supplementary publication no. CCDC-1511738 and 1495799, respectively. Copies of the data can be obtained upon application to CCDC, 12 Union Road, Cambridge CB2 1EZ, UK (Fax: +44 1223/336033; e-mail: deposit@ccdc.cam.ac.uk).

Acknowledgement

This work was supported by grant MAT 2015-70615-R from the Spanish Government and by Feder funds. Funded by the CERCA Program / Generalitat de Catalunya. ICN2 is supported by the Severo Ochoa program from Spanish MINECO (Grant No. SEV-2013-0295).

References:

[1] J.-M. Lehn, Supramolecular chemistry, Vch, Weinheim, 1995.

[2] J.-C. Dai, X.-T. Wu, Z.-Y. Fu, C.-P. Cui, S.-M. Hu, W.-X. Du, L.-M. Wu, H.-H. Zhang, R.-Q. Sun, Synthesis, structure, and fluorescence of the novel cadmium (II)− trimesate coordination polymers with different coordination architectures, Inorganic chemistry, 41 (2002) 1391-1396.

[3] O.M. Yaghi, H. Li, C. Davis, D. Richardson, T.L. Groy, Synthetic strategies, structure patterns, and emerging properties in the chemistry of modular porous solids, Accounts of Chemical Research, 31 (1998) 474-484.

[4] M.E. Kosal, K.S. Suslick, Microporous porphyrin and metalloporphyrin materials, Journal of Solid State Chemistry, 152 (2000) 87-98.

[5] M.-L. Tong, H.-J. Chen, X.-M. Chen, Molecular Ladders with Multiple Interpenetration of the Lateral Arms into the Squares of Adjacent Ladders Observed for $[M_2(4, 4^{/}\text{-bpy})_3(H_2O)_2(phba)_2](NO_3)_2.4H_2O$ (M= Cu^{2+} or Co^{2+}; 4,4/-bpy= 4,4 '-Bipyridine; phba= 4-Hydroxybenzoate), Inorganic chemistry, 39 (2000) 2235-2238.

[6] P.J. Stang, B. Olenyuk, Self-assembly, symmetry, and molecular architecture: Coordination as the motif in the rational design of supramolecular metallacyclic polygons and polyhedra, Accounts of chemical research, 30 (1997) 502-518.

[7] T.C. Mak, Q. Li, Novel inclusion compounds with urea/thiourea/selenourea-anion host lattices, Advances in Molecular Structure Research, 4 (1998) 151-226.

[8] M.M. Lee, H.-Y. Kim, I.H. Hwang, J.M. Bae, C. Kim, C.-H. Yo, Y. Kim, S.-J. Kim, Cd II MOFs Constructed Using Succinate and Bipyridyl Ligands: Photoluminescence and Heterogeneous Catalytic Activity, Bull. Korean Chem. Soc, 35 (2014) 1777.

[9] O. Yaghi, H. Li, T. Groy, Construction of porous solids from hydrogen-bonded metal complexes of 1, 3, 5-benzenetricarboxylic acid, Journal of the American Chemical Society, 118 (1996) 9096-9101.

[10] O.R. Evans, W. Lin, Pillared, 3D metal-organic frameworks with rectangular channels. Synthesis and characterization of coordination polymers based on tricadmium carboxylates, Inorganic chemistry, 39 (2000) 2189-2198.

[11] L. Pan, N. Ching, X. Huang, J. Li, Reactions and Reactivity of Co− bpdc Coordination Polymers (bpdc= 4, 4/-biphenyldicarboxylate), Inorganic chemistry, 39 (2000) 5333-5340.

[12] H.J. Choi, M.P. Suh, Self-assembly of molecular brick wall and molecular honeycomb from nickel (II) macrocycle and 1, 3, 5-benzenetricarboxylate: guest-dependent host structures, Journal of the American Chemical Society, 120 (1998) 10622-10628.

[13] G.B. Gardner, D. Venkataraman, J.S. Moore, S. Lee, Spontaneous assembly of a hinged coordination network, (1995).

[14] P. Hayati, A.R. Rezvani, A. Morsali, P. Retailleau, Ultrasound irradiation effect on morphology and size of two new potassium coordination supramolecule compounds, Ultrasonics sonochemistry, 34(2017)195-205.

[15] G.B. Deacon, P.W. Felder, P.C. Junk, K. Müller-Buschbaum, T.J. Ness, C.C. Quitmann, The X-ray crystal structures of [Hg(C_6F_4OH-p)$_2$ OH_2] and [Hg(C_6H_4OMe-p)($O_2CC_6F_4$ OMe-p)]–factors influencing supramolecular Hg–O interactions, Inorganica chimica acta, 358(2005)4389-4393.

[16] H. Lee, M. Diaz, C.B. Knobler, M.F. Hawthorne, Octahedral coordination of an iodide ion in an electrophilic sandwich, Angewandte Chemie, 112 (2000) 792-794.

[17] W.-T. Chen, M.-S. Wang, X. Liu, G.-C. Guo, J.-S. Huang, Investigations of Group 12 (IIB) Metal Halide/Pseudohalide-Bipy Systems: Syntheses, Structures, Properties, and TDDFT Calculations (Bipy= 2,2′-bipyridine or 4,4′-bipyridine), Crystal growth & design, 6 (2006) 2289-2300.

[18] G. Mahmoudi, A. Morsali, A.D. Hunter, M. Zeller, Mercury (II) coordination polymers generated from 1, 4-bis (2 or 3 or 4-pyridyl)-2, 3-diaza-1, 3-butadiene ligands, CrystEngComm, 9 (2007) 704-714.

[19] M.C. Bernini, F. Gándara, M. Iglesias, N. Snejko, E. Gutiérrez- Puebla, E.V. Brusau, G.E. Narda, M. Monge, Reversible Breaking and Forming of Metal–Ligand Coordination Bonds:

Temperature-Triggered Single-Crystal to Single-Crystal Transformation in a Metal–Organic Framework, Chemistry-A European Journal, 15 (2009) 4896-4905.

[20] J.H. Bang, K.S. Suslick, Sonochemical synthesis of nanosized hollow hematite, Journal of the American Chemical Society, 129 (2007) 2242-2243.

[21] P. Hayati, A.R. Rezvani, A. Morsali, P. Retailleau, S. García-Granda, Influences of temperature, power ultrasound and reaction time on the morphological properties of two new mercury (II) coordination supramolecular compounds, Ultrasonics sonochemistry, 34 (2017) 968-977.

[22] J.H. Bang, K.S. Suslick, Applications of ultrasound to the synthesis of nanostructured materials, Advanced materials, 22 (2010) 1039-1059.

[23] K.S. Suslick, M. Fang, T. Hyeon, Sonochemical synthesis of iron colloids, Journal of the American Chemical Society, 118 (1996) 11960-11961.

[24] K.S. Suslick, D.J. Flannigan, Inside a collapsing bubble: sonoluminescence and the conditions during cavitation, Annu. Rev. Phys. Chem., 59 (2008) 659-683.

[25] S.M. van der Meer, B. Dollet, M.M. Voormolen, C.T. Chin, A. Bouakaz, N. de Jong, M. Versluis, D. Lohse, Microbubble spectroscopy of ultrasound contrast agents, The Journal of the Acoustical Society of America, 121 (2007) 648-656.

[26] H. Xu, B.W. Zeiger, K.S. Suslick, Sonochemical synthesis of nanomaterials, Chemical Society Reviews, 42 (2013) 2555-2567.

[27] M.J.S. Fard, P. Hayati, A. Firoozadeh, J. Janczak, Ultrasonic synthesis of two new zinc (II) bipyridine coordination polymers: New precursors for preparation of zinc (II) oxide nano-particles, Ultrasonics sonochemistry, 35 (2017) 502-513.

[28] I. Wharf, T. Gramstad, R. Makhija, M. Onyszchuk, Synthesis and vibrational spectra of some lead (II) halide adducts with O-, S-, and N-donor atom ligands, Canadian Journal of Chemistry, 54 (1976) 3430-3438.

[29] P. Hayati, A. Rezvani, A. Morsali, P. Retailleau, R. Centore, Survey of temperature, reaction time and ultrasound irradiation power on sonochemical synthesis of two new nanostructured lead (II) coordination supramolecule compounds, Ultrasonics sonochemistry, 35 (2017) 81-91.

[30] P. Hayati, A.R. Rezvani, A. Morsali, D.R. Molina, S. Geravand, S. Suarez-Garcia, M.A.M. Villaecija, S. García-Granda, R. Mendoza-Meroño, P. Retailleau, Sonochemical synthesis, characterization, and effects of temperature, power ultrasound and reaction time on the morphological properties of two new nanostructured mercury (II) coordination supramolecule compounds, Ultrasonics Sonochemistry, 37 (2017) 382-393.

[31] L. Shimoni-Livny, J.P. Glusker, C.W. Bock, Lone pair functionality in divalent lead compounds, Inorganic Chemistry, 37 (1998) 1853-1867.

[32] M.J.S. Fard, P. Hayati, H.S. Naraghi, S.A. Tabeie, Synthesis and characterization of a new nano lead (II) 0-D coordination supramolecular compound: A precursor to produce pure phase nano-sized lead (II) oxide, Ultrasonics Sonochemistry, 39 (2017) 129-136.

[33] Z.H. Chohan, M. Praveen, A. Ghaffar, Structural and biological behaviour of Co (II), Cu (II) and Ni (II) metal complexes of some amino acid derived Schiff-bases, Metal-Based Drugs, 4 (1997) 267-272.

[34] F. Marandi, K. Moeini, S. Ghasemzadeh, Z. Mardani, C.K. Quah, W.-S. Loh, Synthesis, spectral and X-ray diffraction of two new 2D lead (II) coordination polymers formed by nicotinic acid N-oxide linkers, Journal of Molecular Structure, (2017).

[35] N. Rad-Yousefnia, B. Shaabani, M. Kubicki, M.S. Zakerhamidi, A.M. Grzeskiewicz, 2D holodirected lead (II) halide coordination polymers based on rigid N, N′-bis (4-pyridylmethylidyne) phenylene-1, 4-diamine ligand: Syntheses, crystal structures, NBO studies and luminescence properties, Polyhedron, 129 (2017) 38-45.

[36] S.J. Musevi, E. Şahin, A. Aslani, Synthesis of PbO and PbBr 2 nanopowders from nano-sized 2D lead (II) coordination polymers, Powder technology, 229 (2012) 30-36.

[37] Y.-Q. Chen, Y. Tian, Lead (II) coordination polymers based on rigid-flexible 3, 5-bis-oxyacetate-benzoic acid: Structural transition driven by temperature control, Journal of Solid State Chemistry, 247 (2017) 60-66.

[38] A. Aslani, A. Morsali, V.T. Yilmaz, O. Büyükgüngör, 2D Holodirected lead (II) bromide coordination polymers constructed of rigid and flexible ligands, Inorganica Chimica Acta, 362 (2009) 1506-1510.

[39] A. Aslani, A. Morsali, V.T. Yilmaz, C. Kazak, Hydrothermal and sonochemical synthesis of a nano-sized 2D lead (II) coordination polymer: A precursor for nano-structured PbO and PbBr 2, Journal of Molecular Structure, 929 (2009) 187-192.

[40] L. Saghatforoush, A. Bakhtiari, H. Gheleji, Synthesis, X-ray crystal structure, optical properties and DFT studies of a new 2D layered iodide bridged Pb (II) coordination polymer with 2, 3-bis (2-pyridyl) pyrazine, Journal of Solid State Chemistry, 221 (2015) 433-440.

[41] J.-D. Lin, C.I. Onet, W. Schmitt, Photoluminescent lead (II) coordination polymers stabilised by bifunctional organoarsonate ligands, Science and technology of advanced materials, 16 (2015) 024803.

[42] Rigaku (2014) CrystalClear-SM expert 2.1b43 The Woodlands, Texas, USA, and Rigaku Corporation, Tokyo, Japan.

[43] Sheldrick, G. M. (2015). Acta Cryst. A71, 3-8.

[44] Spek, A. L. (2009). Acta Cryst. D65, 148–155.

[45] SADABS, Bruker-Nonius, Delft, The Netherlands, 2002.

[46] A. Altomare, M. C. Burla, M. Camalli, G. L. Cascarano, C. Giacovazzo, A. Guagliardi, G. G. Moliterni, G. Polidori, R. Spagna, J. Appl. Crystallogr. 32 (1999) 115-119.

[47] G. M. Sheldrick, Acta Crystallogr. A64 (2008) 112-122.

[48] L. J. Farrugia, J. Appl. Crystallogr. 45 (2012) 849-854.

[49] Mercury 1.4.1, Copyright Cambridge Crystallographic Data Centre, 12 Union Road, Cambridge, CB2 1EZ, UK, 2001–2005.

[50] V.A. Blatov, A.P. Shevchenko, D.M. Proserpio, Applied topological analysis of crystal structures with the program package ToposPro, Crystal Growth & Design, 14 (2014) 3576-3586, http://topospro.com.

[51] E.V. Alexandrov, V.ABlatov, A.Kochetkov, D.M.Proserpio, Underlying nets in three-periodic coordination polymers: topology, taxonomy and prediction from a computer-aided analysis of the Cambridge Structural Database, CrystEngComm, 13 (2011) 3947-3958.

[52] O.V. Dolomanov, L.J. Bourhis, R.J. Gildea, J.A. Howard, H. Puschmann, OLEX2: a complete structure solution, refinement and analysis program, Journal of Applied Crystallography, 42 (2009) 339-341.

Table 1. Crystal data and structures refinement for $[Pb_2(L)_2(Br)_2]_n.H_2O$ **(1)**, $[Pb_2(HL^{/})(L^{/})(H_2O)_2]_n \cdot H_2O$ (**2**).

Empirical formula	**$C_{12}H_8Br_2N_2O_4Pb_2 \cdot 0.5(H_2O)$ (1)**	**$C18H_{13}O_{15}Pb_2$ (2)**
Formula weigh	827.41 g/mol	**883.68 g/mol**
Temperature	296(2)K	**293(2)K**
Wavelength	0.71073 Å	**0.71073 Å**
Crystal system	Monoclinic	**Triclinic**
Space group	$P2_1/n$	P_{-1}
Unit cell dimensions	a = 8.6303 (7) Å,α=90.000(5)° b = 8.5930 (7)Å, β =99.576 (5)° c = 23.0762(19) Å,γ =90.000 (5)°	a =9.3156 (17)Å,α=67.764 (9)° b = 10.268 (2)Å,β=85.707 (10)° c = 12.893 (3)Å,γ =71.778 (9)°
Volume	1687.5 (2)$Å^3$	1083.0(4) $Å^3$
Z	4	2
Density(calculated)	3.257 g/cm^3	2.734 g/cm^3
Absorption coefficient	24.683 Mg/m^3	0.343 Mg/m^3
F(0 0 0)	1460	810
Theta range for data collection	2.5 to 25.6°	2.9 to 28.6°
μ Index ranges	24.68 mm^{-1} $-11 \leq h \leq 9$ $-11 \leq k \leq 11$ $-27 \leq l \leq 29$	15.61 mm^{-1} $-12 \leq h \leq 12$ $-13 \leq k \leq 13$ $-17 \leq l \leq 17$
$(\sin \theta/\lambda)max$	0.650 $Å^{-1}$	0.674 $Å^{-1}$
Theta(max)	25.6°	28.6°
Radiation type Refinement method Goodness- of- fit on F^2	Mo Kα Full–matrix least–squares on F^2 1.021	Mo Kα Full–matrix least–squares on F^2 1.042
Refinement	$R[F^2 > 2\sigma(F^2)]=0.036$ $wR(F^2)=0.083$ S=1.02	$R[F^2 > 2\sigma(F^2)]=0.041$ $wR(F^2)=0.078$ S=1.04
R1 [I>2σ(I)]	15082, 3834, 2848	24099, 6412, 5072
Rint Largest diff. peak and hole CCDC no.	0.064 1.58 and -1.58 eA^{-3} 1511738	0.073 2.35, -198 eA^{-3} 1495799

Table 2. Selected bond lengths/ Aº for compound $[Pb_2(L)_2(Br)_2]_n \cdot H_2O$ (**1**)

Br(1)—Pb(1)	3.131(1)	C(8)—C(9)	1.393(14)
Br(1)—Pb(2)	3.1482(10)	C(9)—H(9)	0.9300
Br(2)—Pb(1)	3.0815(10)	C(9)—C(10)	1.360(13)
Br(2)—Pb(2)	3.1874(10)	C(10)—H(10)	0.9300
C(1)—H(1)	0.9300	C(10)—C(11)	1.368(11)
C(1)—C(2)	1.378(12)	C(11)—C(12)	1.517(11)
C(1)—N(1)	1.338(10)	O(3)—Pb(1)^{ii}	2.587(6)
C(2)—H(2)	0.9300	O(3)—Pb(2)	2.458(6)
C(2)—C(3)	1.379(14)	Pb(1)—O(3)^{iii}	2.587(6)
C(3)—H(3)	0.9300	Pb(2)—O(1)^{iv}	2.551(6)
C(3)—C(4)	1.425(13)	Pb(2)—O(2)^{iv}	2.701(6)

Symmetry transformations used to generate equivalent atoms:

(i) 1.5-x, -0.5+y, 0.5-z; (ii) 0.5-x, 0.5+y, 0.5-z; (iii) 0.5-x, -0.5+y, 0.5-z; (iv) 1.5-x, 0.5+y, 0.5-z.

Table 3. Selected bond lengths/ Aº for compound $[Pb_2(HL')(L')(H_2O)_2]n \cdot H_2O$ (**2**)

Pb(1)—O(4)	2.516(6)	O(3)—C(7)	1.252(9)
Pb(1)—O(16)	2.530(8)	C(9)—C(1)	1.503(10)
Pb(1)—O(1)	2.567(5)	C(17)—C(12)	1.513(9)
Pb(1)—O(2)	2.664(5)	C(12)—C(11)	1.394(11)
Pb(1)—O(3)	2.717(6)	C(12)—C(13)	1.398(11)
Pb(2)—O(10)	2.505(5)	C(16)—C(10)	1.510(11)
Pb(2)—O(7)	2.532(5)	C(1)—C(6)	1.393(11)
Pb(2)—O(1)	2.544(6)	C(1)—C(2)	1.395(11)
Pb(2)—O(13)	2.610(7)	C(7)—C(5)	1.504(11)
Pb(2)—O(9)	2.633(6)	C(18)—C(14)	1.484(10)

Table 4. The influence of temperature, reaction time, concentration of initial reactant and sonication power on the size of compounds 1 and 2 particles. The ultrasounds power used in all reactions was 60 W.

Synthesis for complex **1**	M(mol/l)[a]	T(°C)[b]	t (min)[c]
1 - 1	0. 1	30	30
1 - 2	0. 1	30	60
1 - 3	0. 1	60	30
Synthesis for complex **2**	M(mol/l)[a]	T (°C)[b]	t (min)[c]
2 - 1	0.01	30	30
2 - 2	0.01	30	60
2 - 3	0.01	60	30

[a] Concentration of initial reactant, [b] Reaction temperature, [c] Reaction time, [d] Average diameter (nm)

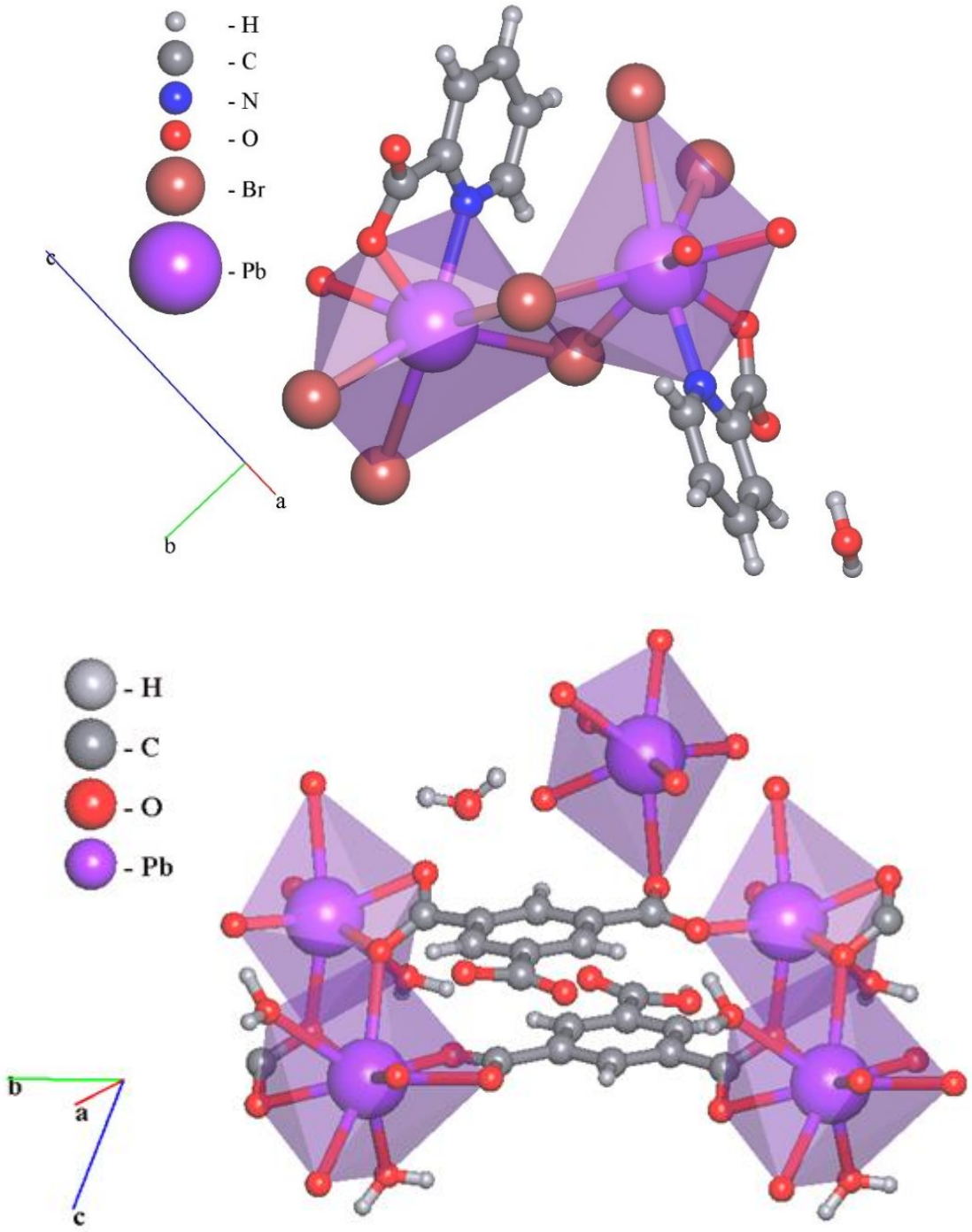

Figure 1. The coordination environment of Pb^{+2} cation environment in complexes (**1**) (up) and (**2**) (down), respectively.

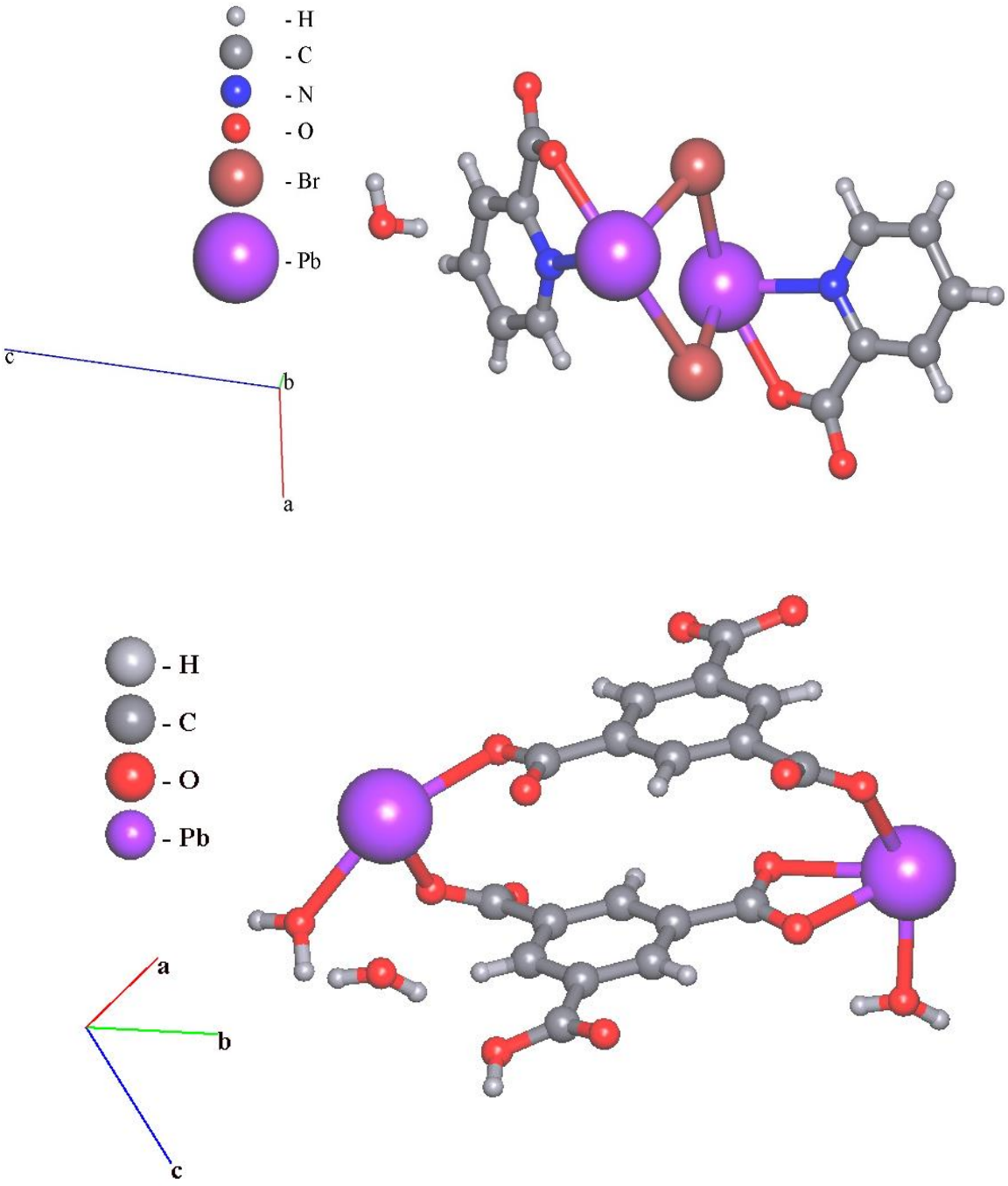

Figure 2. Asymmetric units complexes (**1**) (up) and (**2**) (down), respectively.

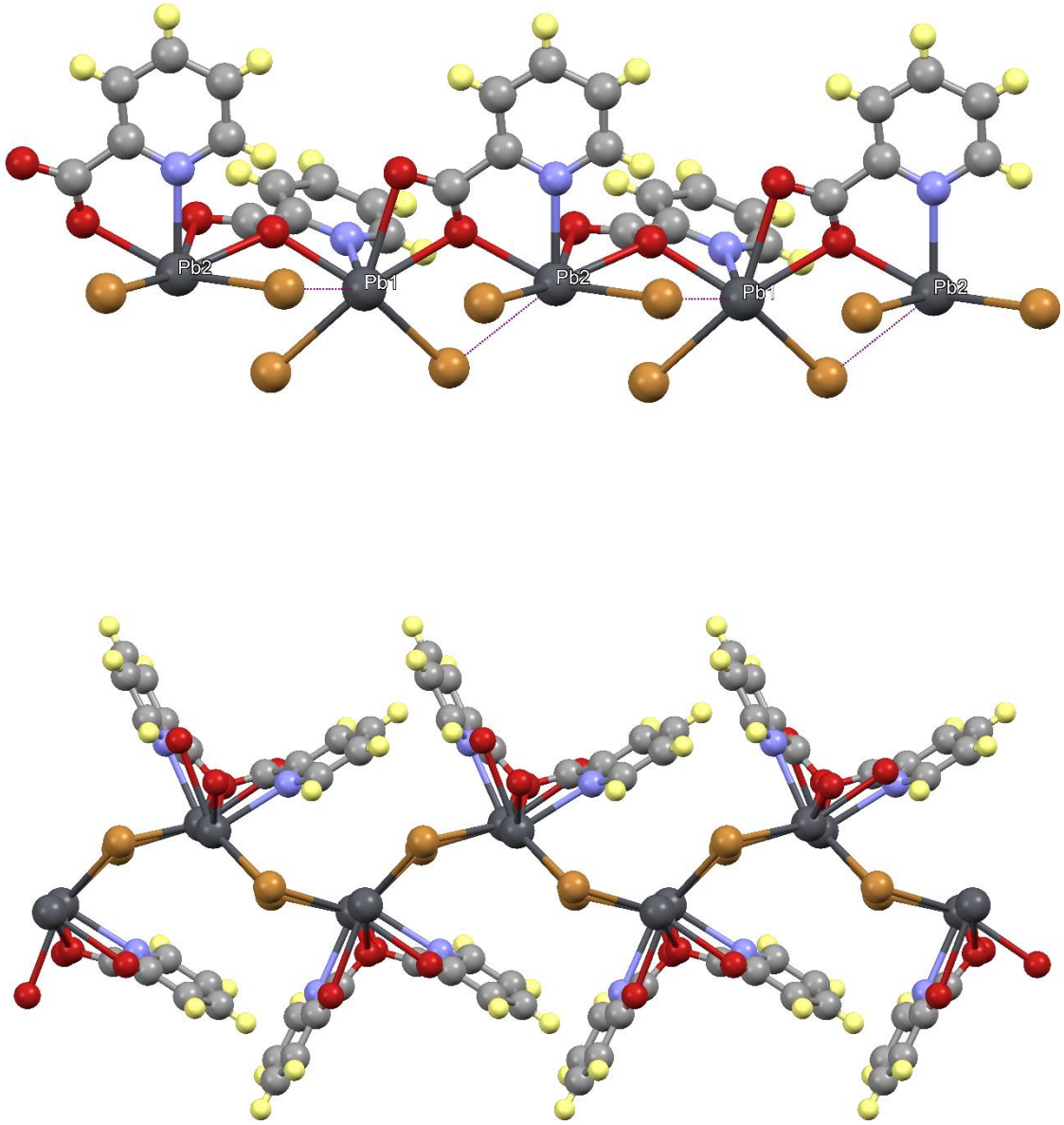

Figure 3. Views of complex (**2**), representation of coordination ligand binding along *a* direction (up), representation of coordination bridging ligand in 2D network along *b* direction (down).

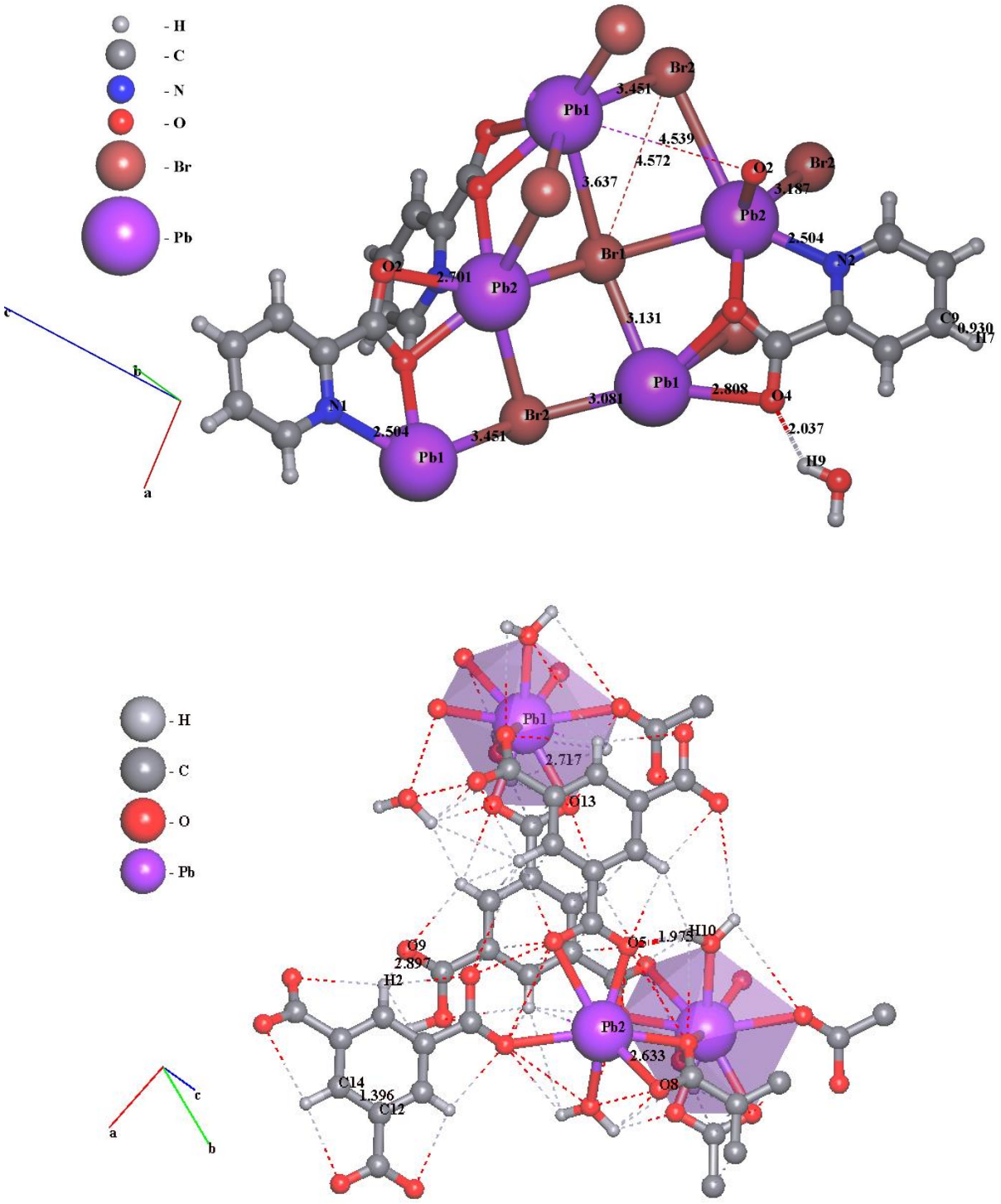

Figure 4. Distance of bound in complexes (**1**) (up) and (**2**) (down).

.

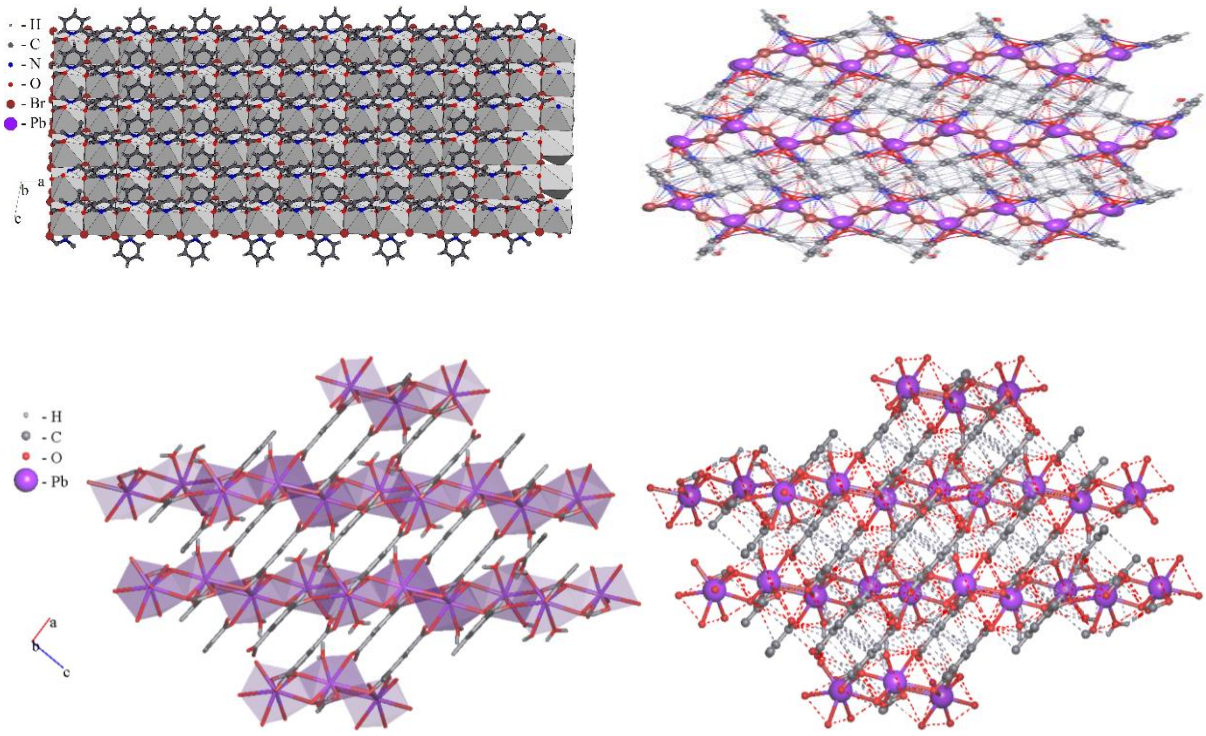

Figure 5. 2D layers of complexes (**1**) and (**2**) (left). Interaction between layers in complexes (**1**) and (**2**) (right).

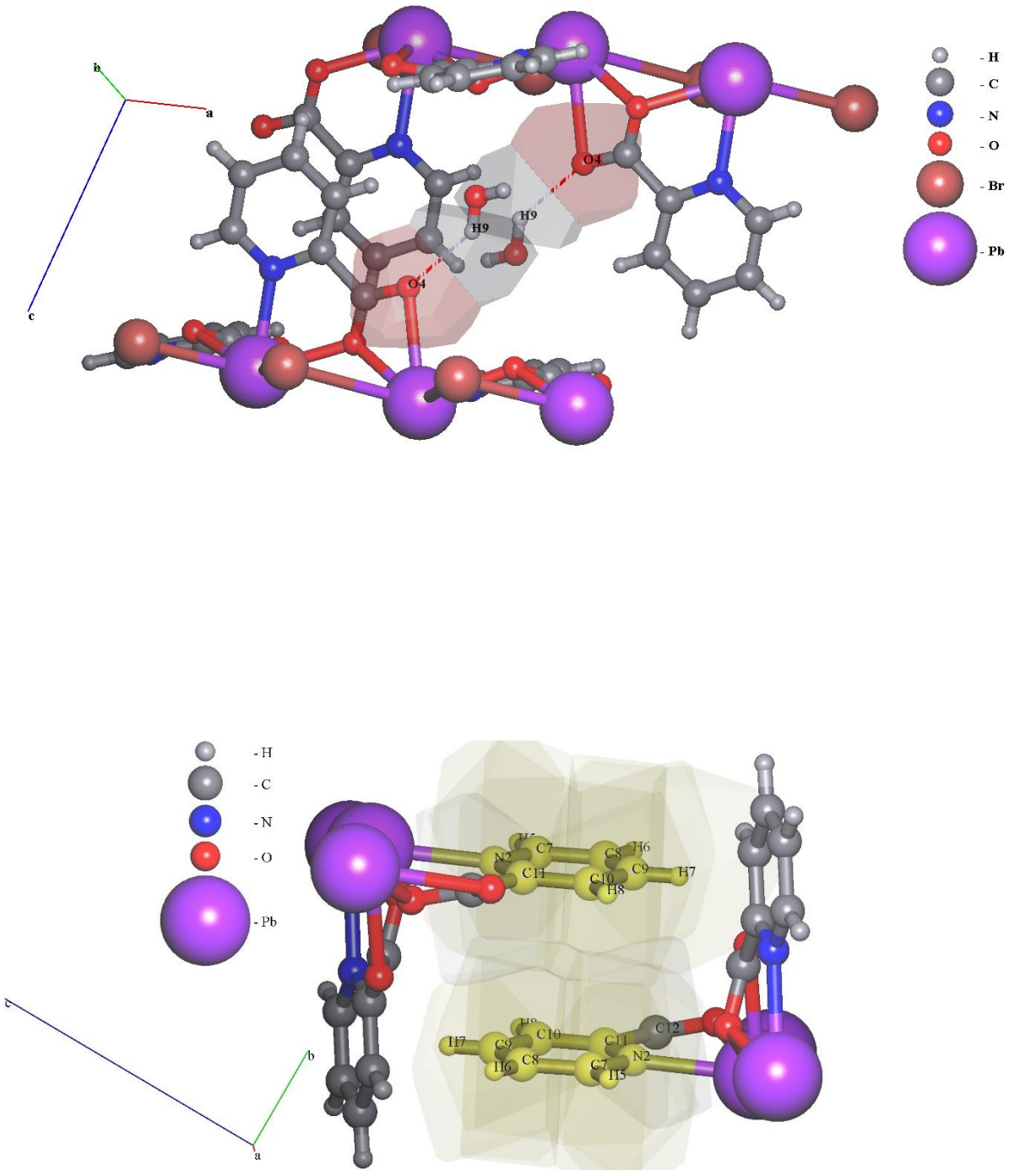

Figure 6. Hydrogen bound and $\pi - \pi$ interaction in complex (**1**).

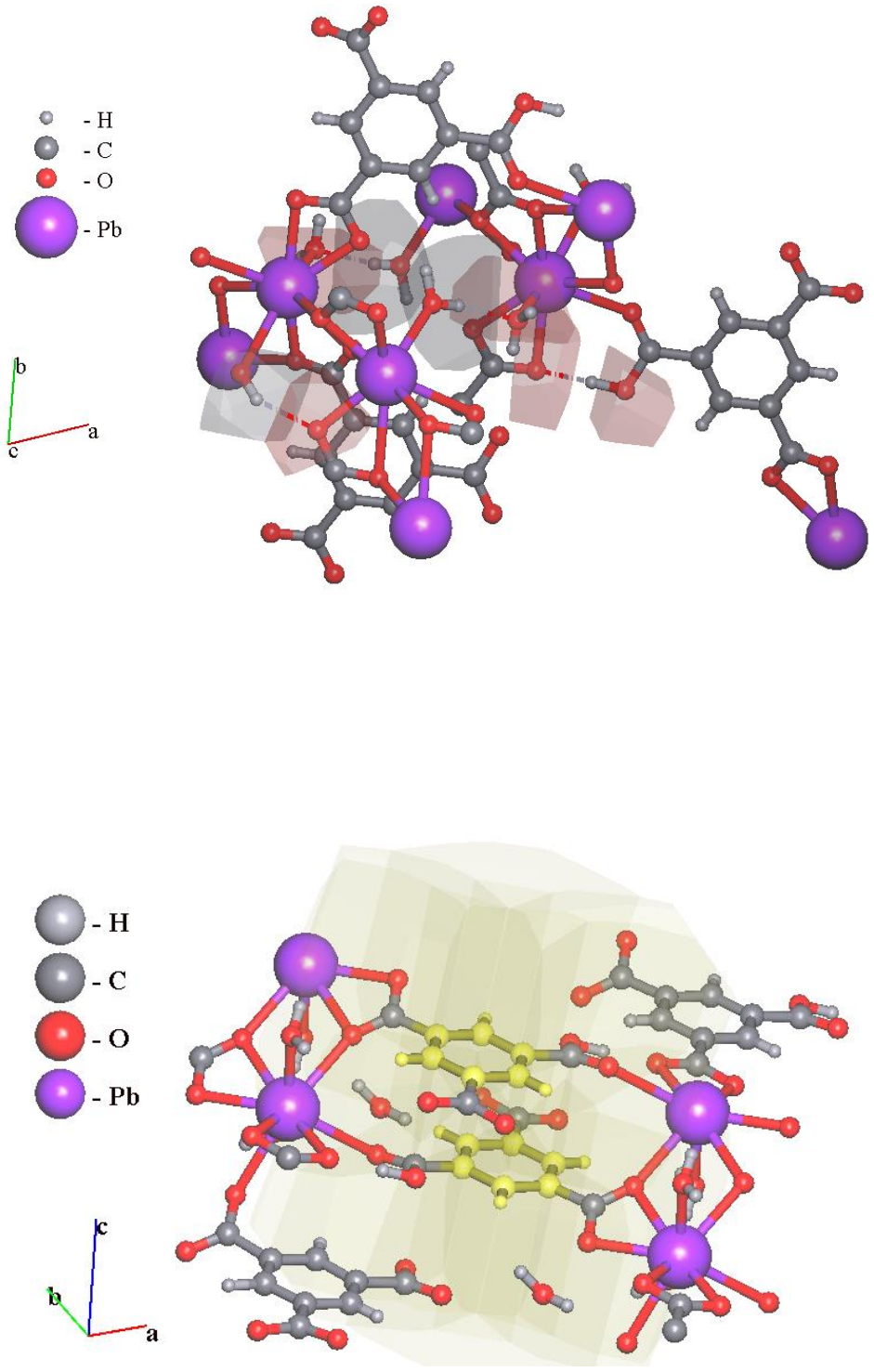

Figure 7. Hydrogen bound and $\pi - \pi$ interaction in complex (**2**).

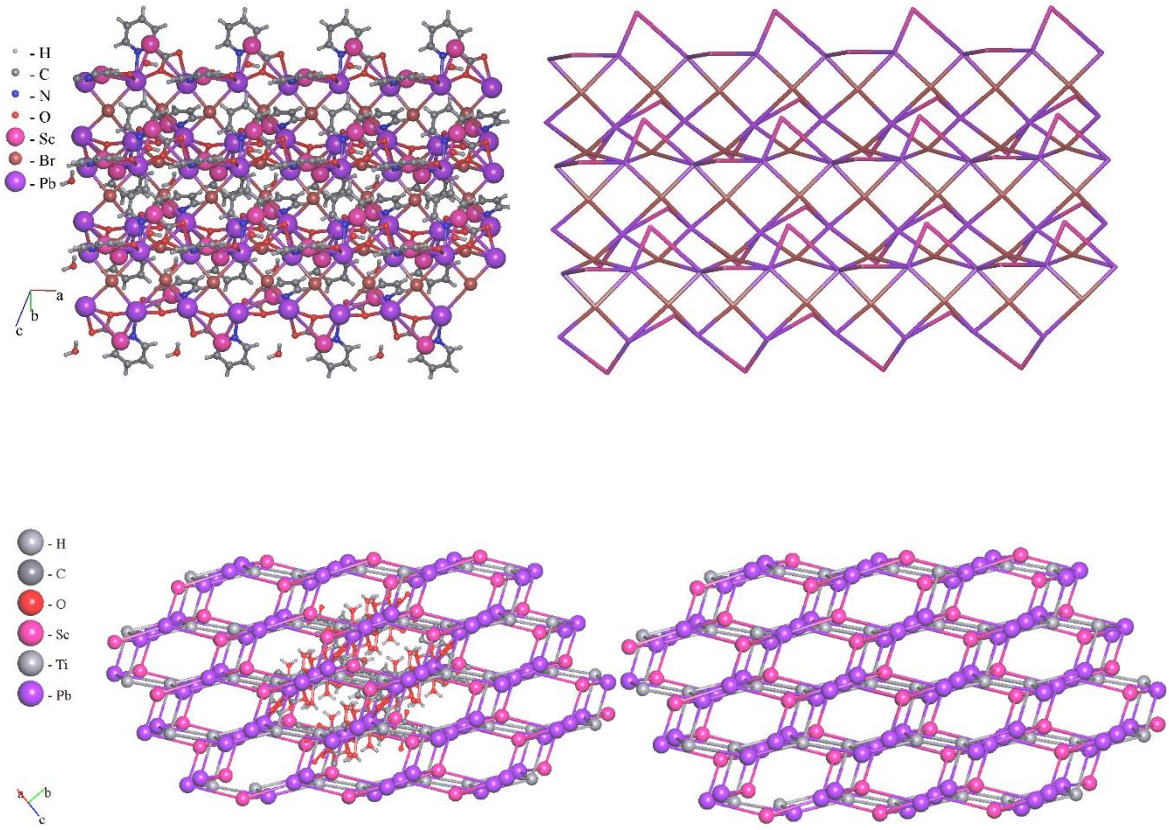

Figure.8. Topological representation of coordination networks in complexes (**1**) (up) and (**2**) (down).

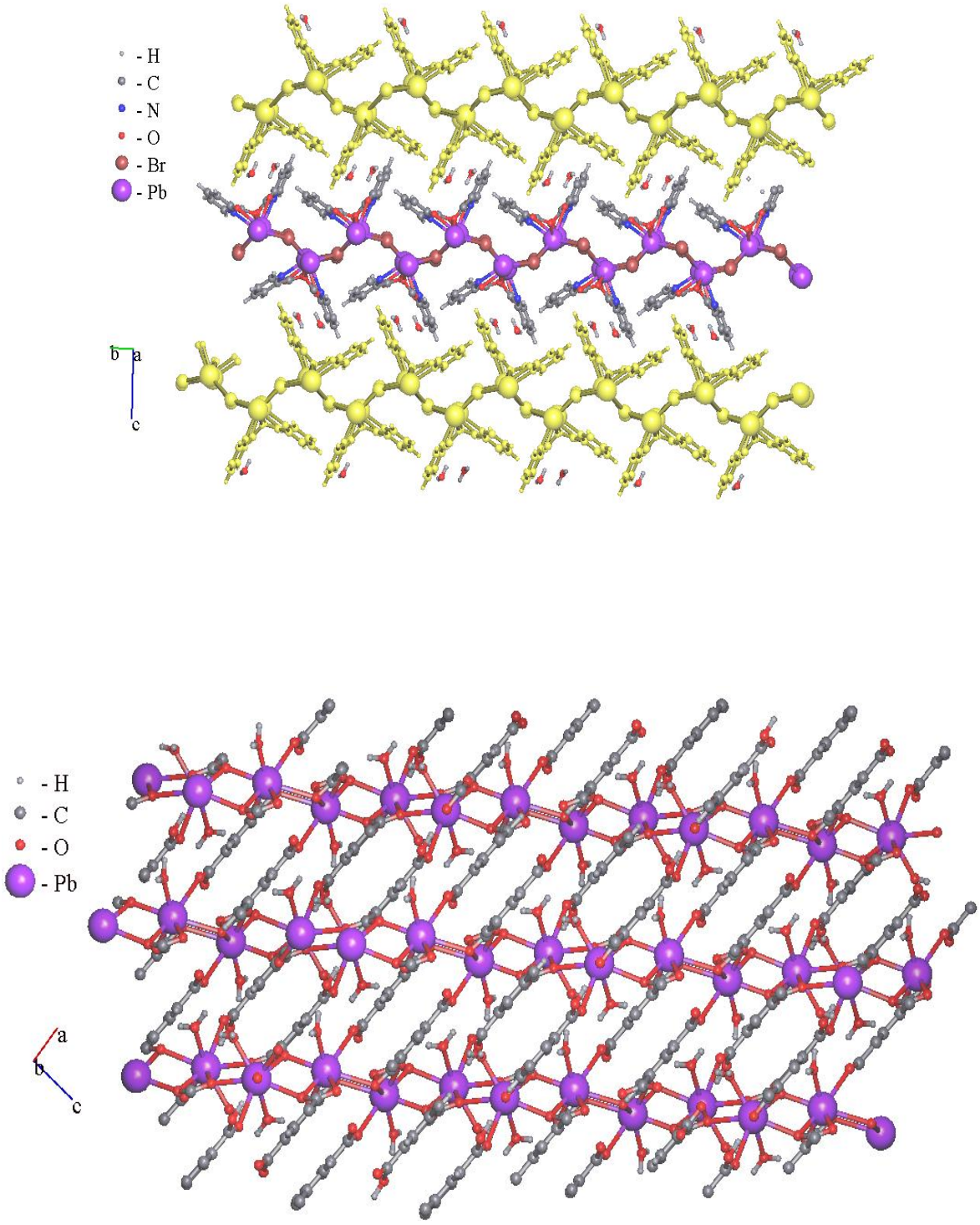

Figure 9. The number of layer, molecules and chain surrounding the complexes (**1**) (up) and (**2**) (down).

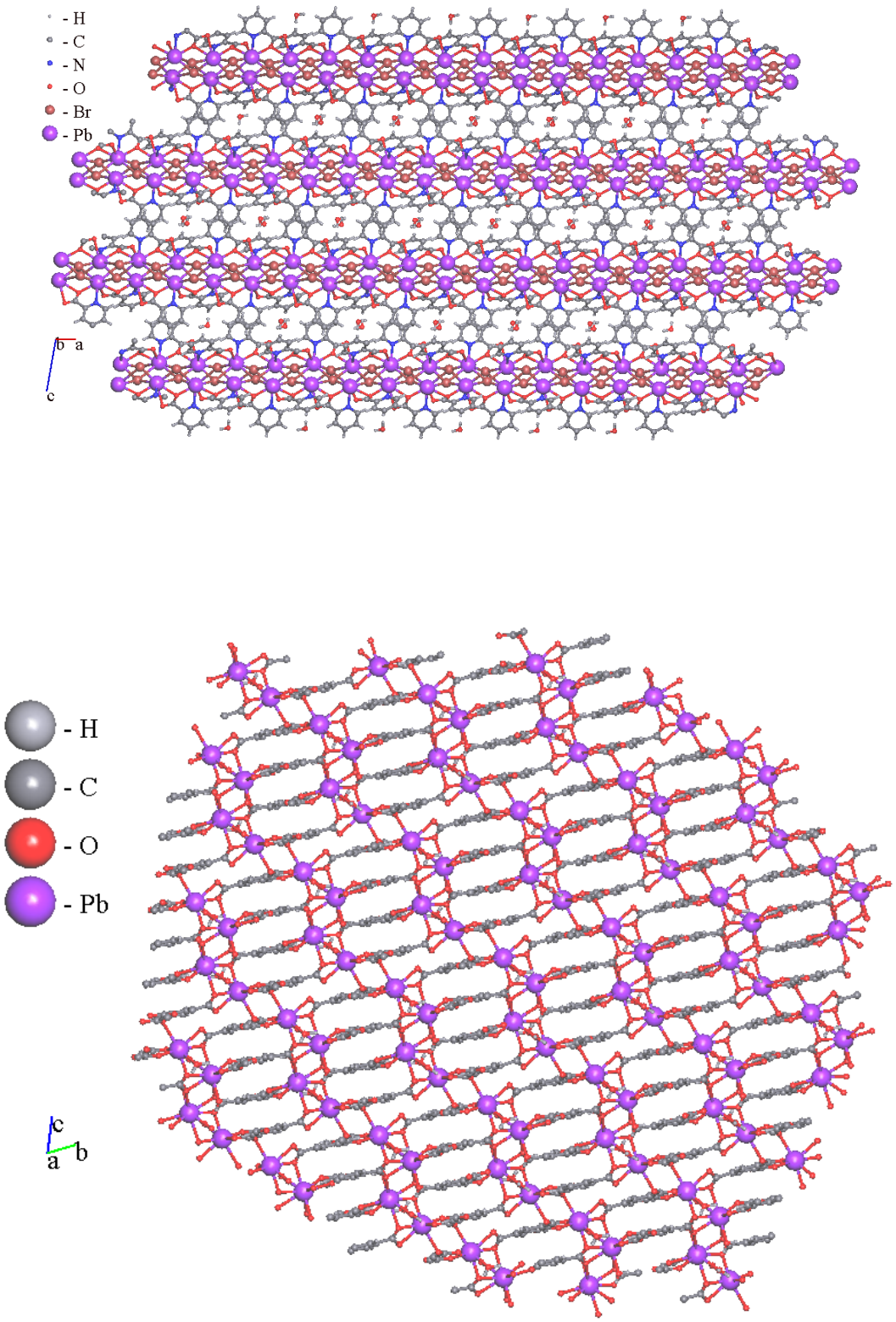

Figure 10. A fragment of the 3D framework in complexes (**1**) (up) and (**2**) (down).

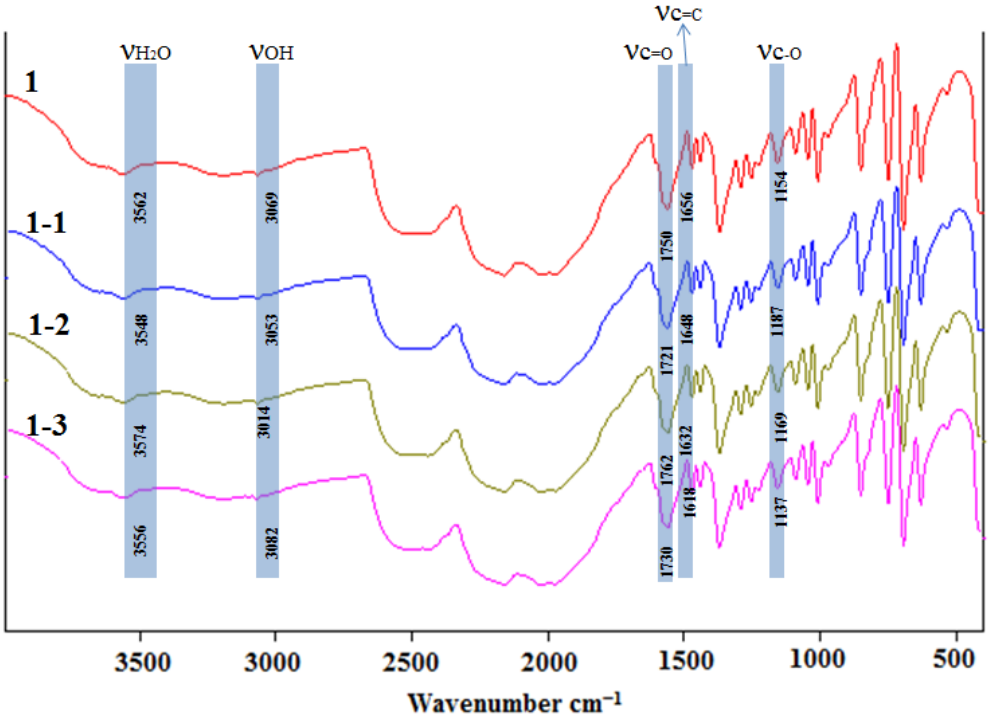

Figure 11. FT-IR spectra of (a) micro-structured **1-1**, **1-2** and **1-3**

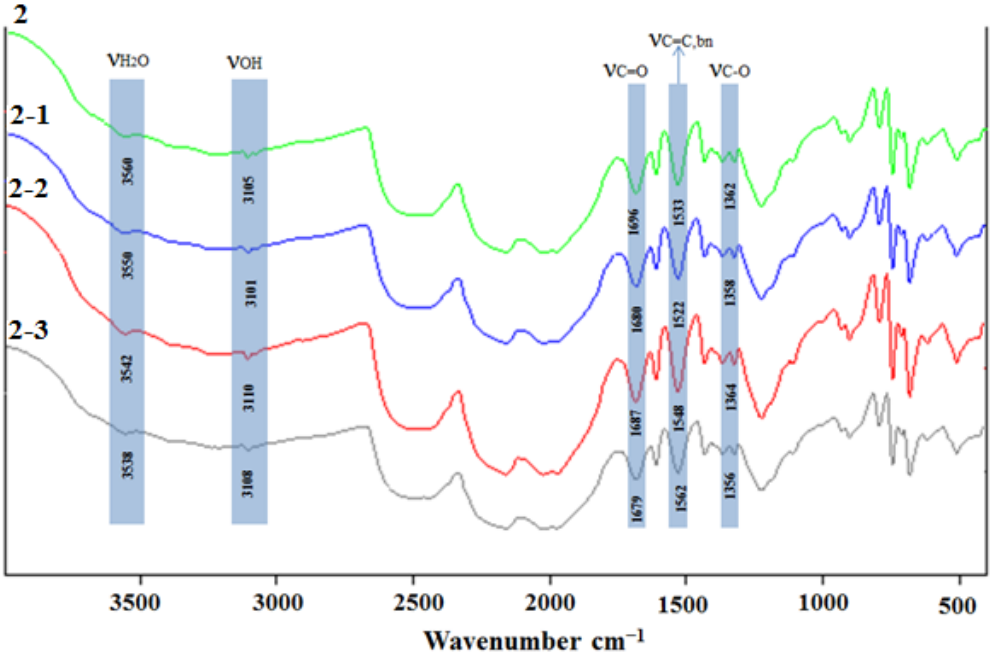

Figure 12. FT-IR spectra of (a) micro-structured **2-1**, **2-2** and **2-3**

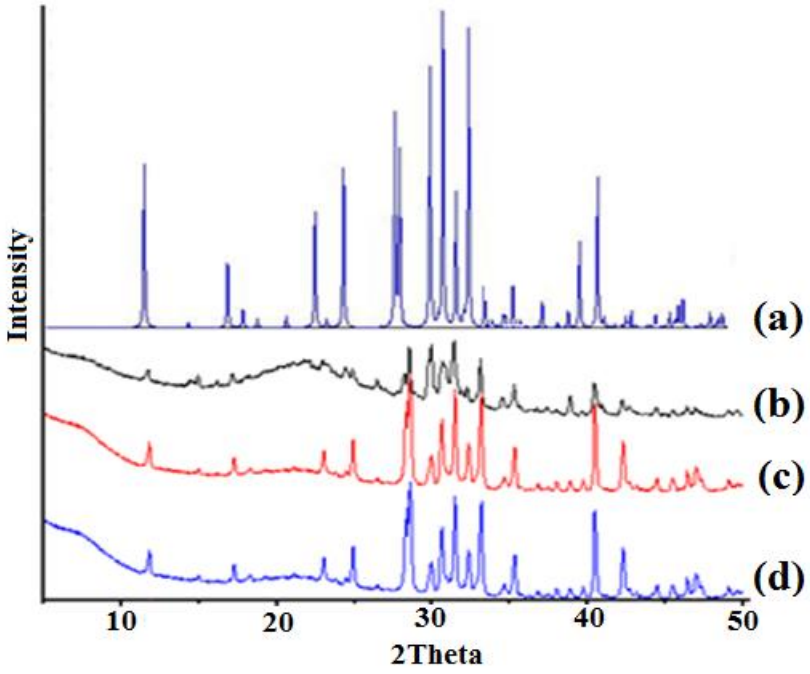

Figure 13. (a) XRD pattern simulation of $Pb_3O_2Br_2$; XRD patterns of $Pb_3O_2Br_2$ which is prepared by calcination of 1-1 (b) 1-2 (c) 1-3(d) at 700°C.

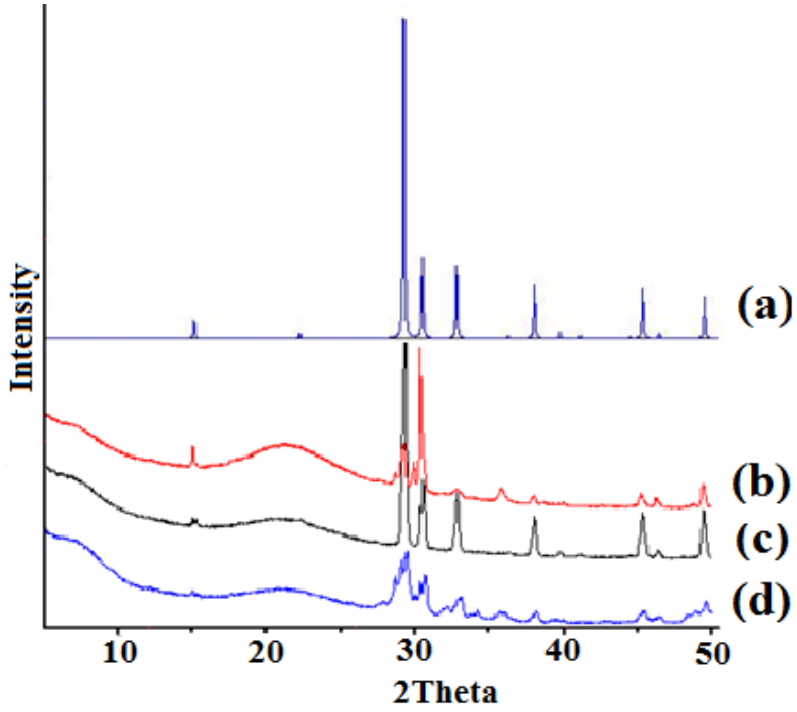

Fig. 14. (a) XRD pattern simulation of PbO; XRD patterns of PbO which is prepared by calcination of 1-1 (a) 1-2 (b) and 1-3 (c) at 700°C.

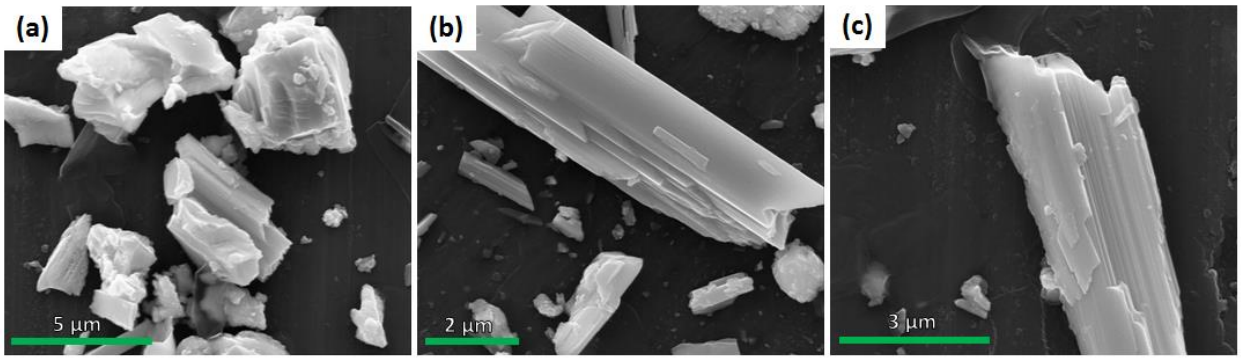

Figure 15. SEM image of PbO which is prepared by calcination of (a) 1-1, (b) 1-2 and (c) 1-3at 700°C.

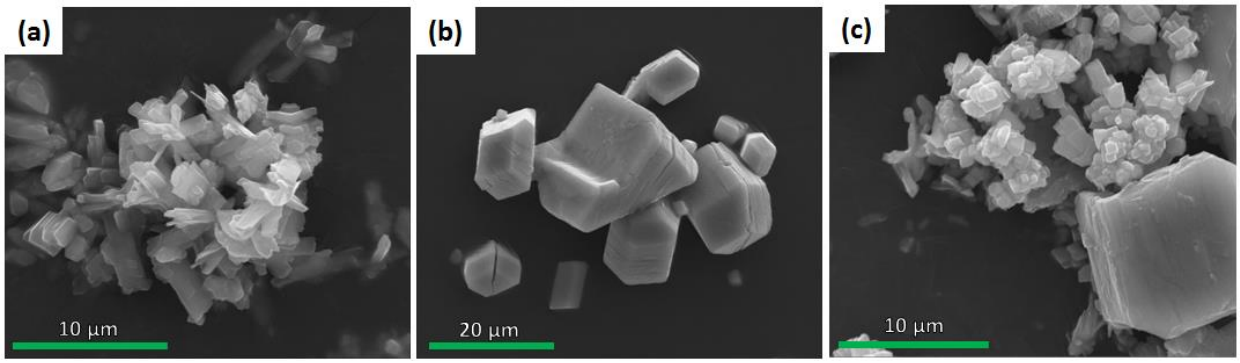

Figure 16. SEM image of PbO which is prepared by calcination of 2-1 (c) 2-2 (d) 2-3 at 700°C.